This is the peer reviewed version of the following article: S. Fredrich, A. Bonasera, V. Valderrey, S. Hecht, *J. Am. Chem. Soc.* **2018**, *140* (*20*), 6432–6440, which has been published in final form at https://pubs.acs.org/doi/10.1021/jacs.8b02982. This article may be used for non-commercial purposes in accordance with ACS Publication Terms and Conditions for Self-Archiving. Supporting Information is available free of charge following the previous link.

# Sensitive Assays by Nucleophile-Induced Rearrangement of Photoactivated Diarylethenes

Sebastian Fredrich, Aurelio Bonasera, Virginia Valderrey and Stefan Hecht*

## Abstract

Upon light-induced isomerization, diarylethenes (DAEs) equipped with reactive aldehyde moieties rearrange selectively in the presence of amines, accompanied by decoloration. In a comprehensive study, the probe structure was optimized with regard to its inherent reactivity in the nucleophile-triggered rearrangement reaction. Detailed structure−reactivity relationships could be derived, in particular with regard to the type of integrated (het)aryl moieties as well as the location of the formyl residue, and the probes' intrinsic reactivity with primary and secondary amines was optimized. Utilizing an ancillary base, the initially formed rearrangement product can engage in a subsequent catalytic cycle, leading to an amplified decoloration process. This additional catalytic pathway allows us to enhance the sensitivity of our method and successfully discriminate between amines and thiols. Moreover, probes that exhibit strong analyte-induced fluorescence modulation have been designed to further decrease the detection limit by using a more sensitive read-out. The optimized DAE probes are promising molecular components for future programmable sensing materials and devices.

## Introduction

The qualitative discrimination and quantification of specific molecular entities plays a crucial role in understanding and monitoring physiological processes. Amines are, for example, involved in important biological regulation mechanisms, such as dopamine in the stimulation/inhibition of potassium channels. [1] Similarly, thiols occupy a prominent role in molecular biology, ranging from the formation of stabilizing disulfide cross-links in α-keratin [2] to the prevention of oxidative stress and the coenzymatic role in several reactions with glutathione.[3,4] Nevertheless, various amines and thiols are connected to pathological conditions, for instance dopamine present during different stages of Parkinson's disease.[5]

In addition to the specific nature of the (bio)analytes, their concentration is another key parameter to survey. [6] Industrial effluvia in potable water sources or food spoilage can be harmful when the concentration of

biogenic amines overcomes a certain limit. [7] Consequently, the presence of these amino compounds is indicative of insufficient hygiene conditions [8] and potential toxicological effects. [9] Biogenic amines, found in a wide range of foods, most notably meat and fish, consist of low-volatile amines formed via thermal or enzymatic decarboxylation of amino acids by bacteria. [10-12] Examples include ethanolamine, spermidine, spermine, and the most widely studied cadaverine, histamine, and putrescine, produced by decarboxylation of lysine, histidine, and ornithine, respectively. [11] Volatile sulfur compounds (VSCs) are another important class of analytes in food chemistry and increasing attention has been paid to their organoleptic relevance. [13] They arise from common sulfur-containing precursors, in particular methionine. [14]

Routine laboratory techniques of quantifying biogenic amines and thiols are mainly based on chromatography coupled with mass spectrometry. [15-17] Because of their high-costs and complexity, simpler tools for analyte evaluation in food matrices were recently established. Although most rely on ordinary colorimetric assays, [18-23] the limit of color perception is only challenged in a few examples where catalytic/enzymatic mechanisms further decrease the detection limit. [24-25]

Among colorimetric assays, approaches using fluorescence detection exhibit significant advantages. [26-28] Complex matrices often comprise a high background color that needs to be considered, whereas fewer samples show autofluorescence or quenching. This latter effect can be used to determine the concentration of certain analytes via Stern−Volmer analysis using fluorescent dyes that respond to amino groups. [29] Other techniques exploit turn-on fluorescence by reacting the analyte with a sensor molecule to generate a highly emissive product or to shift its emission maximum. [27, 28, 30-32]

In order to externally control the operation of the sensor, approaches have been developed using photochromic compounds to regulate the detection of amino acids, cyanide anions, thiols, organophosphorus compounds, and other analytes. [18,19,33-37] In most of these “smart” assays, the added optical switching feature plays a major role due to the existence of one inactive state while the other is able to probe the desired analyte. Recently, we reported diarylethene (DAE) single-component probes, which undergo facile decoloration in the presence of amines after light-induced activation. [38] The remote-control over reactivity is remarkable and allows to store the dormant probe for long time, even in an environment contaminated with the analyte. Despite these advantages, we wanted to lower the detection limit and clarify some details of the mechanism. This motivated us to lead our new studies into four main directions: (i) investigation of different structural motifs, in order to understand key structural parameters that could improve sensitivity and speed (Figure 1); (ii) detailed insight into the sensing mechanism, including the different reactivities of the involved species; (iii) application of the thus optimized molecular systems to selectively and efficiently recognize various classes of biomolecules, providing a unique tool for multiple-targets trace sensing; (iv) utilization of the specific spectral features of the inactive, active, and neutralized forms to create turn-on sensors with high optical sensitivity.

In this article, we report a comprehensive investigation of the structure−reactivity relationships of aldehyde-substituted DAE probes deciphering the influence of the position of the reactive carbonyl moiety as well as the nature of substituents on the response to amines and thiols. On the basis of our detailed mechanistic understanding, we describe two approaches, namely catalytic amplification and fluorescence read-out, to

discriminate between amine and thiol analytes and increase the overall sensitivity of our remote-controlled detection systems.

## Results and discussion

## Synthesis

In order to identify the most sensitive probe, i.e., the molecular structure with the highest photoinduced reactivity toward the analyte, several structural variations were synthesized and subsequently explored (Scheme 1). For synthesis, different heterocycles were equipped with formyl groups using metalation by *n*-BuLi followed by reaction with dimethylformamide (DMF). The aldehyde function was masked as an acetal before further functionalization by Suzuki coupling to give rise to a large variety of precursors (Schemes S1 and S2). Assembly of the majority of the target DAEs was achieved by sequential reaction of the metalated heteroaromatic building blocks to perfluorocyclopentene followed by deprotection under acidic workup conditions (see Schemes S3−S7). [39] An analogous synthesis was used to prepare phenyl-substituted DAEs **7** and **8** (see Scheme S6). Note that synthesis of indole-substituted DAEs **10**/**11** as well as **19** required N-protection by a *tert*-butyloxycarbonyl (BOC) group. Preparation of the benzothiophene-bridged DAEs **16**−**18** was realized using two separate cross-coupling reactions (see Scheme S8). Further details about the synthesis and characterization data can be found in the Supporting Information.

## Structure−Reactivity Relationships.

In order to have a fair comparison, the compound showing the best performance in our initial work, [38] DAE-**O**, was used as benchmark. As typical for DAEs, the open isomer **Oo** absorbs only in the UV-region ($\lambda_{max}$ = 285 nm) and undergoes 6π-electrocyclization upon UV-light irradiation ($\lambda_{irr}$ = 365 nm), indicated by purple coloration of the solution and the rise of a new spectral band ($\lambda_{max}$ = 580 nm) in the visible range (Figure 2, red line). According to chromatographic analysis of the final irradiated solution, the photostationary state (PSS) contains about 85% of the closed isomer **Oc**. Irradiation with visible light ($\lambda_{irr}$ > 500 nm) leads to full recovery of the open isomer **Oo**. This switching process can be repeated over several cycles. The addition of *n*-octylamine (OA) to the solution of pure **Oo** does not have any relevant effect for several weeks, when some amount of the corresponding imine **Ooi** is being formed, which can be switched reversibly to its closed form **Oci**. On the contrary, the irradiated mixture containing **Oc** immediately undergoes decolouration when OA is added, resulting in a yellowish solution (Figure 2, blue line). We thus concluded that the closed isomer is involved in an irreversible rearrangement reaction, producing the photoinactive compound **Or**. A reasonable mechanism for the observed rearrangement reaction evokes the initial nucleophilic attack of the amine to the highly reactive, aliphatic aldehyde of the closed DAE, resulting in the corresponding hemiaminal intermediate. Subsequently, this intermediate rearranges to the more stable compound **Or** accompanied by formation of N-octylformamide (Figure 2, top).

On the basis of these previous findings, the first new design we decided to investigate concerned DAE compounds with aldehyde groups in the outer part of the molecular skeleton (see series I in Figure 1).[40] For an easy comparison of the general behaviour and sensing capacities, these molecules have a similar design, only exchanging the phenyl substituents in the parent DAE-**O** by aldehydes in the periphery and bearing two methyl groups at the ring-closing inner α-position of the molecule (see DAEs **1** and **2** in Scheme 1). These DAEs preserve the general features described by our group in a different context for compounds with non fluorinated bridge. [40] While in the presence of an excess of amine (OA, $4.0 \times 10^{-2}$ M) **Oc** is completely transformed into the rearrangement product in less than 3 min, its positional analogue 1c does not undergo any rearrangement but instead is fully condensed into the corresponding imine **1ci** in around 20 h (see Figure S56). As expected, the imine can be switched back and forward by means of visible and UV-light irradiation, respectively, without inducing irreversible changes of the molecular scaffold (Figure 3). We rationalize these findings by considering that upon ring-closure the aromatic aldehyde group experiences only a slight modulation of its electronic nature and thus reactivity toward amines. More importantly, the intermediate hemiaminal is inactive toward rearrangement, in strong contrast to the one formed in case of **Oc**. Similarly, the reactivity of the symmetrical compound **2** with two aldehyde moieties at the periphery was found analogous.

Once we confirmed the necessity of positioning the aldehyde functionality in the core position to enable an effective rearrangement, we introduced two formyl groups in the two inner α-thienyl positions of the DAE structure. The resulting symmetrical derivative **3** should in principle exhibit a higher probability of reacting with amines. However, upon irradiation of **3o** with UV-light the generation of two new species, the expected closed isomer **3c**, but also another compound with inferior mass, i.e., **3r**, was observed (see Figure S25). Isolation and characterization by UV/vis spectroscopy (see Figure S54 and Table S7), HRMS, $^{1}$H and $^{19}$F NMR revealed that the formed **3r** is no longer switchable and resembles the structure of the other rearrangement products. In a control experiment, an irradiated mixture containing **3o**, **3c**, and **3r**, was monitored in the darkness, but even after 2 h, no (further) transformation of **3c** to **3r** was observed (see Table S3). Thus, our hypothesis to explain these findings assumes that continued irradiation of (photogenerated) **3c** with UV-light triggers the rearrangement event, even in the absence of amine.

After establishing one formyl group in the core of the DAE structure to be optimal, we evaluated the effect of different substituents in the outer phenyl pendants (see series II in Figure 1). As long as no competing aldehyde is located there, the mechanism of the rearrangement should not differ from the one as shown in Figure 2. The rearrangement is presumably driven by formation of the aromatic central 6-membered ring as well as the resonance stabilized formamide and should be accelerated by the presence of electron-withdrawing groups (EWGs). Thus, a trifluoromethyl ($-CF_3$) group was introduced in para-position of the phenyl moiety adjacent to either the aldehyde function to render it more reactive or the opposite thiophene moiety to facilitate its breakdown (see DAEs **4** and **5** in Scheme 1). Indeed, photoactivated compound **5c** was found to be more reactive toward amines with rate constants up to 1.6 times larger in the case of spermidine (SPER) when compared to reference **Oc** (Table 1). Placing the EWG closer to the reactive site further accelerated the

rearrangement as the reaction with SPER proceeds at twice the rate of the benchmark switch. In an effort to combine both of these effects, DAE-**6** was synthesized and its closed isomer **6c** rearranges 2.7 times faster than **Oc** in the presence of SPER. A similar tendency was observed for other amines (Table 1) and thus the derived structure−reactivity relationship appears to be general. However, in view of exceptions such as for BA (Table 1) we have refrained from providing general sensitivity factors for the reaction with nonspecified amines.

Though introducing EWGs into the DAE-scaffold clearly enhances the reactivity of the ring-closed aldehydes, this effect is probably weakened by the rather electron-rich thiophene moieties and the substantial distance of the electron-accepting substituents from the reactive centre.

To further optimize the reactivity, we were considering less electron-rich aromatic rings attached directly to the central olefinic bridge and therefore replaced either thiophene moiety by a phenyl ring (see DAEs **7** and **8** in Scheme 1). On the one hand, **7o** bearing a benzaldehyde moiety, upon irradiation gave a variety of products, which we attribute to nonselective photocyclization with regard to the position of ring-closure. On the other hand, changing the opposite thiophene to a phenyl moiety was expected to block the rearrangement due to replacing the weak C−S bond, to be broken, by a stronger C−C bond. To our surprise, addition of amines to solutions containing photogenerated **8c** also led to rapid bleaching of the visible band over a time range comparable with other switches in our library. Puzzled by this result, we were able to isolate the formed rearrangement product, which turned out to be difficult due to a low ratio of **8c** in the PSS caused by its thermal instability at room temperature ($t_{1/2}$ = 4.5 h, see Table S3). A combination of techniques (1D- and 2D $^{1}$H and $^{19}$F NMR experiments, HRMS, see Supporting Information, Figures S20−S22, S55, Table S7) allowed us to determine the chemical structure of **8r**, which is consistent with the assumption that the rearrangement does not involve breaking of a C−C bond within the phenyl residue as described by Ho et al. [41] It seems that despite limited stabilization by the formed cross-conjugated π-system, elimination of HF drives the rearrangement (Figure 4). Computational results support that formation of this unexpected rearrangement product is indeed thermodynamically favoured (see Table S8). Interestingly, the optimized geometry of **8c** exhibits different C−F bond lengths (see Figures S76 and S77 and Table S9), suggesting an enhanced and biased reactivity of the closed isomer (see section 6 in the Supporting Information). The observed rearrangement is related to previous reports involving fluoride elimination of the closed isomer of diarylethenes [42−44] or other pathways, [45, 46] most notably the irreversible thermally bleaching of some oxidized dithienylethenes due to release of $SO_2$. [47−51]

All the above results are in agreement with our proposed mechanism (see Figure 2, top). Clearly, the introduction of EWGs in key positions both enhances the reactivity of the formyl group toward initial nucleophilic attack of the amine analyte and accelerates the rearrangement of the formed intermediate. It appears that resonance stabilization of the aromatic fused benzenes as well as formamide products (or alternatively HF elimination in the case of **8c**) is the main driving force behind the observed rearrangement.

## Catalytic Amplification.

In order to further enhance the sensitivity of our system, we thought of engaging the initially produced rearrangement product in a subsequent catalytic cycle, which would involve nucleophilic attack of its own precursor, thereby accelerating decolouration of the closed DAE probe. However, under neutral conditions explored thus far the formed thiol **Or** appears not to be reactive enough to induce the rearrangement. Thus, we were considering to add a tertiary amine base to deprotonate the formed thiol, thereby greatly enhancing its nucleophilicity. Note that though primary and secondary amines trigger the rearrangement, tertiary amines cannot and therefore should be able to serve solely as the base. On the basis of these considerations, we were exploring basic conditions for the rearrangement, which should initially be triggered by substoichiometric amounts of primary or secondary amine analytes and subsequently be amplified in a catalytic self-decolouration process.

Initial experiments reacting **Oc** with substoichiometric amounts of OA led to partial bleaching of the visible band, corresponding to the amount of amine added. In addition, OA was completely consumed and converted to N-octylformamide. Then, a tertiary amine base, i.e., N,N-dimethylbenzylamine (DMBA) shown to be unreactive by itself, was added in excess, and suddenly the bleaching of the visible band takes place, with a comparable rate yet until complete consumption of **Oc** (see Figure S58), increasing the sensitivity of the probe. This finding strongly supports our reaction mechanism (Figure 5). It is important to note that the overall concentration of nucleophile in solution remains constant, reflecting the level of initially added amine.

In view of this modified, base-catalysed mechanism, we can now explain why after the addition of amine to the closed DAE probe, a small band appears in the absorption spectrum between 400 and 500 nm, which persists until the end of the reaction (see Figure 2, bottom). Upon addition of acid, the band disappears and therefore we attribute it to the thiolate rearrangement product formed due to the basic environment resulting from the nonreacted amine (see Figure S57). This suggest that the catalytic pathway takes place also in the presence of excess of amine, but its contribution to the decolouration velocity is negligible because the concentration of nucleophile is quasi constant under these conditions.

On the basis of the new, more detailed mechanism, we followed three strategies to exploit it in order to enhance the sensitivity of our probes. First, we designed an advanced molecular probe carrying an integrated tertiary amine group with a $pK_a$ similar to DMBA and unable to react by itself with the aldehyde giving a false positive response. However, this new DAE probe **9**, containing a N,N-dimethylamino group at the periphery, exhibited intense fluorescence under irradiation at 365 nm leading to formation of only a negligible amount of ring-closed, activated probe at the PSS. Though a PSS rich in **9c** can be achieved by quenching fluorescence through addition of acid (the corresponding ammonium salt **9-H**$^+$ does not emit, see Figure S30 and Tables S1− S4), it contradicts the idea of an internal base. These findings led to the design of the two DAE probes **10** and **11**, which contain an indole fragment integrated either in regular or inverse fashion, i.e., connected via its 2- and 3-position, respectively. To our surprise, and disappointment, neither **10** nor **11** underwent

photocyclization even after prolonged irradiation times with UV-light in acetonitrile solution. Once again, this problem presumably arising from formation of a twisted intramolecular charge transfer (TICT) state can be circumvented by changing to a nonpolar solvent, [52, 53] such as *n*-hexane in which efficient photo-cyclization is observed (see Figure S31 and Tables S2−S4). Because of the strong solvent dependency of the $pK_a$ of amines and thiols, however, the formation of thiolates in such a nonpolar medium is more difficult to achieve and the presence of one equivalent of the tertiary amine base would presumably not have a significant effect.

After our unsuccessful attempts to design an internally base-assisted probe, we then were aiming to decrease the $pK_a$ of the generated thiol to achieve deprotonation already under neutral conditions. With all previously discussed DAE probes, the rearrangement resembles an ene-thiol and thus we designed **12** carrying a benzothiophene moiety, which after rearrangement gives rise to formation of a more acidic thiophenol. Though the rate of the decolouration reaction is comparable with **Oc**, upon addition of substoichiometric amounts of amine, however, no evidence for a self-induced decolouration of **12c** could be observed (see Figure S71).

Finally, tertiary amine was added right at the start of the decolouration reaction. The setup was slightly changed, employing a cuvette with shorter path length (1 mm) to allow for 1 order of magnitude higher concentrations according to Lambert−Beer Law. Thus, a solution containing our generic DAE probe **Oc** is reacted with substoichiometric amount (less than 0.5 equiv.) of OA in absence and presence of DMBA, respectively (Figure 6). While in the absence of the base, the DAE probe is gradually consumed resulting in a partial decolouration of the sample, the presence of the ancillary base results in a more pronounced bleaching in accordance with the catalytic mechanism. In the absence of primary or secondary amine analyte, the base causes only negligible decolouration.

## Discrimination of Analytes.

In addition to amines, we were interested in expanding the scope of our method to the potential detection of other nucleophiles, in particular alcohols and thiols that represent typical constituents of food matrices as well. On the basis of our above finding that deprotonation appears to be essential to induce sufficient reactivity in the case of thiols and in view of the much higher $pK_a$ values of alcohols as compared to thiols, we were speculating that their discrimination should be possible simply by choosing an appropriate ancillary base.
For these experiments, we decided to explore the more reactive DAE probe **6c** and use DMBA as the base. In two blank experiments, solutions of **6c** were treated with 4-*tert*-butylbenzyl mercaptan and ethanol, respectively. The model thiol was selected as it resembles an aliphatic thiol yet exhibits low volatility and thus an acceptable smell, whereas ethanol was chosen because it is omnipresent in foods and readily available in high purity. In both cases, in the absence of DMBA no decolouration was observed (see Figure S59). In the presence of DMBA, however, addition of the thiol induced bleaching of the visible absorption band and a degradation of **6c**, similarly to what was observed for the catalytic experiments (see Figures S65−67, 74, 75).

This allows us to selectively distinguish between amine and thiol analytes. In other experiments, different quantities of DMBA were used while keeping the concentration of the thiol constant and a linear correlation between basicity and the apparent rate of the decolouration was found (see Figure S68). Cleavage of the thioester formed in the catalytic process (see DAE-**t** in Figure 5) and thus a contribution of subsequently potentially generated thiol/thiolate could be ruled out (see Figure S60). In strong contrast to thiols, the presence of alcohols did not lead to any detectable decolouration and thus rearrangement as the basicity of DMBA is too low to generate alkoxides. Stronger bases capable of deprotonating alcohols, such as sodium hydride and *tert*-butoxide, led to immediate decolouration of the DAE solution, even in the absence of alcohols. Similar negative results were obtained testing for phenol as the prototype of aromatic alcohols. In view of the observed chemoselectivity of decolouration we developed a simple flowchart for discriminating primary/secondary amines from thiols (Figure 7), even in the presence of alcohols.

## Fluorescence Read-Out.

After increasing the reactivity of the DAE probe by optimizing its substitution pattern and implementing an addition al base-catalysed amplification mechanism, we sought to further lower the detection limit by developing a more sensitive read-out. Following the absorbance spectral change of a coloured solution toward bleaching is effective but lacks sensitivity, especially for the naked eye, when compared to the evolution of colour from a noncolored negative sample. As a result, a slight coloration can more readily be observed than a slight decolouration event, giving rise to a lower threshold. When considering a DAE, which is colourless in both, the open and closed isomer but is supposed to be coloured in the rearranged form, the problem is that the latter typically exhibits a hypsochromically shifted absorption maximum as compared to the closed isomer due to its less extended π-system. The solution for this problem is the evolution of a band upon nucleophile addition that is not present in the absorption spectrum.

The DAE probe **14** in both of its switching states as well as its rearranged structure meets these requirements. It comprises on the reactive side a benzothiophene moiety that is converted via nucleophile-induced rearrangement of **14c** into a dibenzothiophene scaffold in **14r** (Figure 8, top). Such structures are known to show a considerable fluorescence, whereas a simple benzothiophene is not emissive. [54, 55] Indeed, **14o** exhibits a very weak and broad emission band at around 580 nm. This emission band disappears completely upon UV-induced ring-closure. Note that residual emission resulting from incomplete ring-closure in the PSS is mostly reabsorbed by the intense visible band of **14c** ($\lambda_{max}$ = 542 nm). Addition of an excess of OA induced rearrangement to give **14r**, accompanied by the rise of a sharp emission band at 365 nm upon excitation at 250 nm (see Figure S48). Thus, one should be able to detect amines with a high sensitivity by directly measuring the amount of rearranged form **14r** via its fluorescence since emission intensity can be considered linear dependent to the concentration at low optical densities (OD < 0.1). [56]

Though the concept of fluorescence detection can be nicely illustrated with DAE probe **14**, the sensitivity of the system is low due to the relatively small fluorescence quantum yield ($\Phi_f$ = 0.007) and the significant emission of the open form. For this reason, alternative structures were considered. Unsubstituted benzothiophene shows slight emission ($\Phi_f$ = 0.019) compared to a barely higher intensity of dibenzothiophene ($\Phi_f$ = 0.08). [54, 55] The more promising related example is benzofuran with negligible fluorescence and dibenzofuran with a much higher fluorescence quantum yield ($\Phi_f$ = 0.53) of its unsubstituted form. [55, 57] Thus, DAE probe **15** bearing a benzofuran moiety was synthesized and, as expected, the colourless acetonitrile solution of the **15o** does not show fluorescence at any excitation wavelength. Upon UV-induced ring-closure, only very weak emission signals appear at around 300 nm when exciting the sample between 200 and 250 nm. Addition of an excess of OA to this sample led to the evolution of an intense emission band centred at 475 nm upon excitation with 400 nm (see Figure S49). Although this example illustrates our design concept and the fluorescence quantum yield ($\Phi_f$ = 0.017) is higher than the one of compound **14**, it is below the maximum that can be reached using this approach.

To boost the sensitivity of our system further, clearly higher fluorescence quantum yields are needed. The structural difference between the open and the rearranged forms of the diarylethenes is the annulated benzene to the aryl ring bearing the aldehyde in the open isomer. In addition, one could imagine replacing the bridge by a unit, which is not fluorescent but after benzene annulation it is. For this purpose, we decided to use a benzothiophene moiety as the bridging unit **45** as well and prepared DAE probe **16**. Indeed, the rearranged form **16r** shows rather intense fluorescence (Figure 8, bottom, $\Phi_f$ = 0.024). The reaction of the closed form **16c** with the amine is, however, significantly slower than for the other investigated DAE probes. This is primarily attributed to the electron-rich character of the benzothiophene bridge when compared to the hexafluorocyclopentene bridging unit, rendering the aldehyde less electrophilic. For this reason, we decided to further modify the connectivity between the reactive and the bridging moieties (see Scheme 1). DAE probe **17**, having an inverted benzothiophene bridge when compared to **16**, shows a slightly slower reaction with OA yet the fluorescence of **17r** is significantly red-shifted ($\lambda_{em}$ = 490 nm, $\lambda_{exc}$ = 370 nm, $\Phi_f$ = 0.025, see Figure S51), which we ascribe to the more planar structure of its bent tribenzodithiophene core. With regard to fluorescence, a combination of a benzothiophene bridge and a benzofuran as the reactive formylated aryl unit appeared attractive. However, DAE probe **18** shows a lower fluorescence quantum yield ($\Phi_f$ = 0.008, see Figure S52) and due to the electron-rich nature of the benzofuran its reactivity is so low that even upon addition of an excess of OA no immediate decolouration occurs.

From the above findings, it is clear that fused heterocycles can induce fluorescence mainly in the rearranged form. Excitation and emission wavelengths are dependent on size and planarity of the fluorophore. While introduction of one heterocycle in the bridge increases the probe's fluorescence efficiency it concomitantly decreases its reactivity. Moreover, breaking overall three aromatic rings upon photocyclization destabilizes the closed isomer leading to deterioration of the photoactivated probe. To overcome this problem, a switch exhibiting the desired analyte-induced fluorescence modulation but constructed using rather electron-poor

building blocks was needed. In this context, we reinvestigated DAE probe **10**, carrying an indole and a thiophene moiety connected via a perfluorocyclopentene bridge. As expected, the open isomer shows a rather intense emission at 390 nm ($\lambda_{exc}$ = 325 nm), which upon ring-closure is bleached until a certain point, reflecting the ratio of open and closed isomers at the PSS.

However, upon addition of OA, a new emission band appears, which is associated with the rearranged form and strongly red-shifted when compared to the one of the open isomer. More importantly, at the excitation maximum of 380 nm the **10o** shows no emission and **10r** can be excited without interference (Figure 9). Moreover, the fluorescence intensity ($\Phi_f$ = 0.03) is the highest among all investigated rearrangement products and the reaction with amines is rather fast, resulting in a high sensitivity of this probe. The only disadvantage is the necessity of using *n*-hexane as solvent to enable UV-induced ring-closure since no photocyclization was observed in acetonitrile. In order to keep the structure as similar to **10** as possible but to improve its switching behaviour in acetonitrile, its BOC-protected precursor molecule **19** was investigated. Gratifyingly, DAE probe **19** is switching in acetonitrile and shows a similar reactivity toward OA as described for **10**. Though the rearrangement product **19r** emits with a slightly lower fluorescence quantum yield ($\Phi_f$ = 0.022, $\lambda_{exc}$ = 320 nm, $\lambda_{em}$ = 440 nm), open and closed isomers do not exhibit any emission (see Figure S53). Therefore, with compounds **10** and **19** we were able to identify appealing probes that allow for fluorescence modulation, either by shifting or turning-on the emission, as an alternative read-out to absorption.

## Conclusion and Outlook.

We were able to identify smart sensor molecules for nucleophile detection as potent probes that can be remotely controlled by light irradiation. Exploring (i) the relationships between DAE structure and photoswitching properties as well as reactivity of the ring-closed form toward an analyte-induced rearrangement, we could ascertain the most effective substitution pattern comprising outer electron-withdrawing groups and inner reactive aldehydes. Moreover, (ii) unravelling of an additional base-catalysed pathway allowed us to lower the detection below the stoichiometric limit and (iii) to successfully discriminate between primary/secondary amines and thiols. Furthermore, (iv) probes with significant analyte-induced fluorescence modulation were designed, allowing us to further enhance the sensitivity of our method. Future work will be concerned primarily with implementation of our DAE probes into actual sensing materials and devices.

### Acknowledgements

V.V. is indebted to the Alexander von Humboldt Foundation for providing a postdoctoral fellowship. Generous support by the European Research Council (ERC via ERC-2012-STG_308117 “Light4Function”), the European Commission (via MSCA-ITN “iSwitch” GA No. 642196), and the German Research Foundation (DFG via SFB 658, project B8) is gratefully acknowledged.

## References


(1) Sasaki, K.; Sato, M. *Nature* **1987**, *325*, 259−262.

(2) Fraser, R. D. B.; MacRae, T. P.; Sparrow, L. G.; Parry, D. A. D. *Int. J. Biol. Macromol.* **1988**, *10*, 106−112.

(3) Meister, A.; Anderson, M. E. *Annu. Rev. Biochem.* **1983**, *52*, 711−760.

(4) Noctor, G.; Foyer, C. H. *Annu. Rev. Plant Physiol. Plant Mol. Biol.* **1998**, *49*, 249−279.

(5) Gingrich, J. A.; Caron, M. G. *Annu. Rev. Neurosci.* **1993**, *16*, 299−321.

(6) Gao, T.; Tillman, E. S.; Lewis, N. S. *Chem. Mater.* **2005**, *17*, 2904−2911.

(7) Bardocz, S. *Trends Food Sci. Technol.* **1995**, *6*, 341−346.

(8) Naila, A.; Flint, S.; Fletcher, G.; Bremer, P.; Meerdink, G. *J. Food Sci.* **2010**, *75*, R139−R150.

(9) Ladero, V.; Calles-Enriquez, M.; Fernandez, M.; Alvarez, M. A. *Curr. Nutr. Food Sci.* **2010**, *6*, 145−156.

(10) Ruiz-Capillas, C.; Jiménez-Colmenero, F.*Crit. Rev. Food Sci. Nutr.* **2005**, *44*, 489−599.

(11) Bulushi, I. A.; Poole, S.; Deeth, H. C.; Dykes, G. A. *Crit. Rev. Food Sci. Nutr.* **2009**, *49*, 369−377.

(12) Roig-Sagues, A. X.; Hernàndez-Herrero, M. M.; López-Sabater, E. I.; Rodríguez-Jerez, J. J.; Mora-Ventura, M. T. *Lett. Appl. Microbiol.* **1997**, *25*, 309−312.

(13) Vermeulen, C.; Gijs, L.; Collin, S. *Food Rev. Int.* **2005**, *21*, 69−137.

(14) Landaud, S.; Helinck, S.; Bonnarme, P. *Appl. Microbiol. Biotechnol.* **2008**, *77*, 1191−1205.

(15) Johnson, D. C.; Dobberpuhl, D.; Roberts, R.; Vandeberg, P. *J. Chromatogr. A* **1993**, *640*, 79−96.

(16) Chesnov, S.; Bigler, L.; Hesse, *M. Eur. J. Mass Spectrom*. **2002**, *8*, 1−16.

(17) Latorre-Moratalla, M. L.; Bosch-Fusté, J.; Lavizzari, T.; Bover-Cid, S.; Veciana-Nogués, M. T.; Vidal-Carou, M. C. *J. Chromatogr. A* **2009**, *1216*, 7715−7720.

(18) Lin, J.-F.; Kukkola, J.; Sipola, T.; Raut, D.; Samikannu, A.; Mikkola, J.-P.; Mohl, M.; Toth, G.; Su, W.-F.; Laurila, T.; Kordas, K. *J. Mater. Chem. A* **2015**, *3*, 4687−4694.

(19) Leng, P. Q.; Zhao, F. L.; Yin, B. C.; Ye, B. C. *Chem. Commun.* **2015**, *51*, 8712−8714.

(20) Rakow, N. A.; Sen, A.; Janzen, M. C.; Ponder, J. B.; Suslick, K. S. *Angew. Chem., Int. Ed.* **2005**, *44*, 4528−4532.

(21) Kumpf, J.; Bunz, U. H. F. *Chem. - Eur. J.* **2012**, *18*, 8921−8924.

(22) Askim, J. R.; Mahmoudi, M.; Suslick, K. S. *Chem. Soc. Rev.* **2013**, *42*, 8649−8682.

(23) Ellman, G. L. *Arch. Biochem. Biophys.* **1959**, *82*, 70−77.

(24) Punakivi, K.; Smolander, M.; Niku-Paavola, M. L.; Mattinen, J.; Buchert, J. *Talanta* **2006**, *68*, 1040−1045.

(25) Wang, Z.; Liu, F.; Lu, C. *Biosens. Bioelectron.* **2014**, *60*, 237−243.

(26) Ueno, T.; Nagano, T. *Nat. Methods* **2011**, *8*, 642−645.

(27) Weigele, M.; DeBernardo, S. L.; Tengi, J. P.; Leimgruber, W. *J. Am. Chem. Soc.* **1972**, *94*, 5927−5928.

(28) Udenfriend, S.; Stein, S.; Böhlen, P.; Dairman, W.; Leimgruber, W.; Weigele, M. *Science* **1972**, *178*, 71.

(29) Rochat, S.; Swager, T. M. *Angew. Chem., Int. Ed.* **2014**, *53*, 9792−9796.

(30) Venkateswarulu, M.; Gaur, P.; Koner, R. R. *Sens. Actuators, B* **2015**, *210*, 144−148.

(31) Mani, P.; Ojha, A. A.; Reddy, V. S.; Mandal, S. *Inorg. Chem.* **2017**, *56*, 6772−6775.

(32) Secor, K. E.; Glass, T. E. *Org. Lett.* **2004**, *6*, 3727−3730.

(33) Mohr, G. J. *Dyes Pigm.* **2004**, *62*, 77−81.

(34) Mertz, E.; Beil, J. B.; Zimmerman, S. C. *Org. Lett.* **2003**, *5*, 3127−3130.

(35) Shao, N.; Jin, J. Y.; Cheung, S. M.; Yang, R. H.; Chan, W. H.; Mo, T. *Angew. Chem., Int. Ed.* **2006**, *45*, 4944−4948.

(36) Shiraishi, Y.; Adachi, K.; Itoh, M.; Hirai, T. *Org. Lett.* **2009**, *11*, 3482−3485.

(37) Shiraishi, Y.; Yamamoto, K.; Sumiya, S.; Hirai, T. *Phys. Chem. Chem. Phys.* **2014**, *16*, 12137−12142.

(38) Valderrey, V.; Bonasera, A.; Fredrich, S.; Hecht, S. *Angew. Chem., Int. Ed.* **2017**, *56*, 1914−1918.

(39) Hanazawa, M.; Sumiya, R.; Horikawa, Y.; Irie, M. *J. Chem. Soc., Chem. Commun.* **1992**, 206−207.

(40) Kathan, M.; Kovaříček, P.; Jurissek, C.; Senf, A.; Dallmann, A.; Thünemann, A. F.; Hecht, S. *Angew. Chem., Int. Ed.* **2016**, *55*, 13882−13886.

(41) Ho, T. I.; Wu, J. Y.; Wang, S. L. *Angew. Chem., Int. Ed.* **1999**, *38*, 2558−2560.

(42) Kobatake, S.; Imagawa, H.; Nakatani, H.; Nakashima, S. *New J. Chem.* **2009**, *33*, 1362−1367.

(43) Lvov, A. G.; Shirinian, V. Z.; Kachala, V. V.; Kavun, A. M.; Zavarzin, I. V.; Krayushkin, M. M. *Org. Lett.* **2014**, *16*, 4532−4535.

(44) Lvov, A. G.; Shirinian, V. Z.; Zakharov, A. V.; Krayushkin, M. M.; Kachala, V. V.; Zavarzin, I. V. *J. Org. Chem.* **2015**, *80*, 11491−11500.

(45) Galangau, O.; Nakashima, T.; Maurel, F.; Kawai, T. *Chem. - Eur. J.* **2015**, *21*, 8471−8482.

(46) Lvov, A. G.; Shirinyan, V. Z. *Chem. Heterocycl. Compd.* **2016**, *52*, 658−665.

(47) Shoji, H.; Kobatake, S. *Chem. Commun.* **2013**, *49*, 2362−2364.

(48) Shoji, H.; Kitagawa, D.; Kobatake, S. *New J. Chem.* **2014**, *38*, 933−941.

(49) Kitagawa, D.; Kobatake, S. *Chem. Lett.* **2011**, *40*, 93−95.

(50) Delbaere, S.; Berthet, J.; Shiozawa, T.; Yokoyama, Y. *J. Org. Chem.* **2012**, *77*, 1853−1859.

(51) Kodama, R.; Sumaru, K.; Morishita, K.; Kanamori, T.; Hyodo,K.; Kamitanaka, T.; Morimoto, M.; Yokojima, S.; Nakamura, S.; Uchida, K. *Chem. Commun.* **2015**, *51*, 1736−1738.

(52) Irie, M.; Sayo, K. *J. Phys. Chem.* **1992**, *96*, 7671−7674.

(53) Herder, M.; Pätzel, M.; Grubert, L.; Hecht, S. *Chem. Commun.* **2011**, *47*, 460−462.

(54) Seixas de Melo, J.; Rodrigues, L. M.; Serpa, C.; Arnaut, L. G.;Ferreira, I. C. F. R.; Queiroz, M. J. R. P. *Photochem. Photobiol.* **2003**, *77*, 121−128.

(55) Nijegorodov, N.; Luhanga, P. V. C.; Nkoma, J. S.; Winkoun, D. P. *Spectrochim. Acta, Part A* **2006**, *64*, 1−5.

(56) Miller, J. N. *Standards in fluorescence spectrometry*; Chapman and Hall, **1981**.

(57) Tero, T.-R.; Salorinne, K.; Lehtivuori, H.; Ihalainen, J. A.; Nissinen, M. *Chem. - Asian J.* **2014**, *9*, 1860−1867.

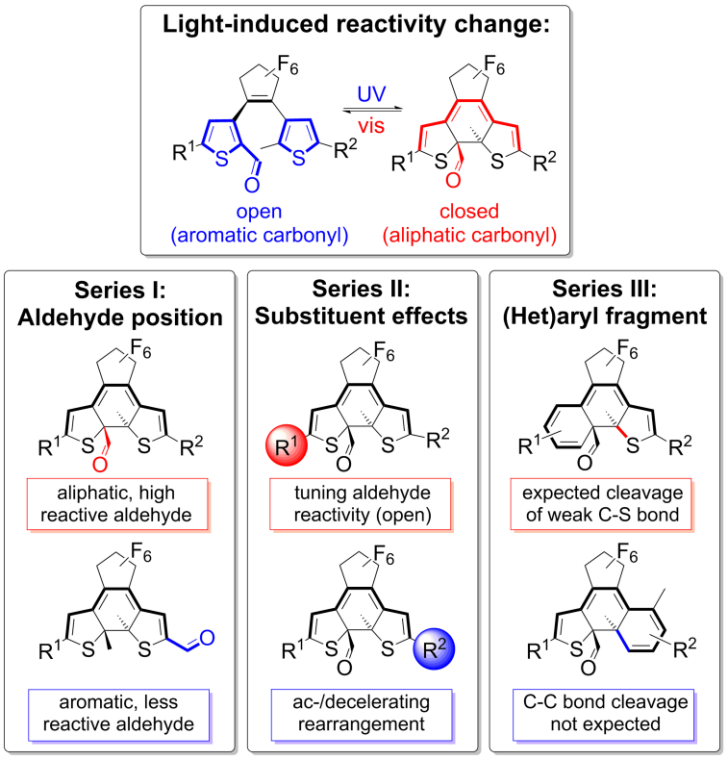


**Figure 1.** Light-induced reactivity modulation of diarylethene aldehyde probes towards nucleophiles.

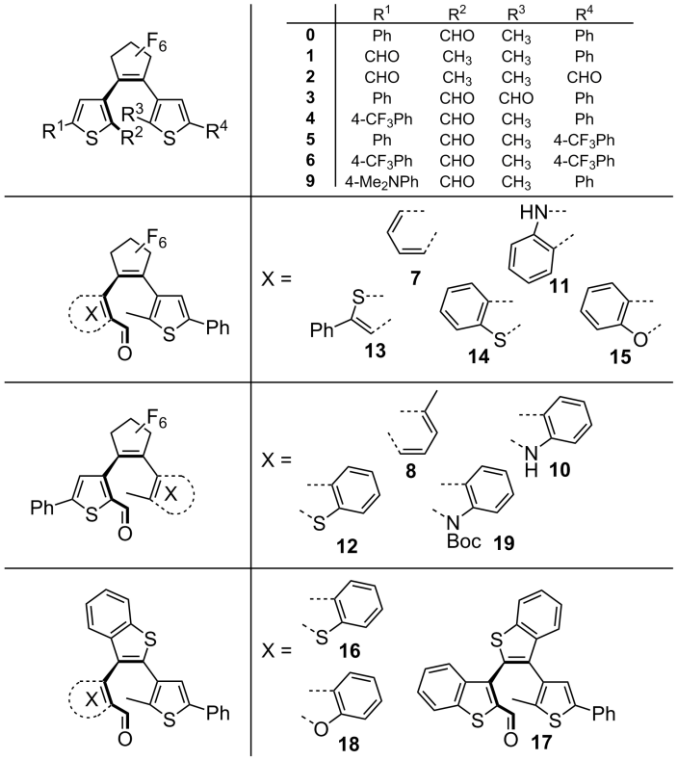


**Scheme 1.** Overview of the investigated DAE probes.

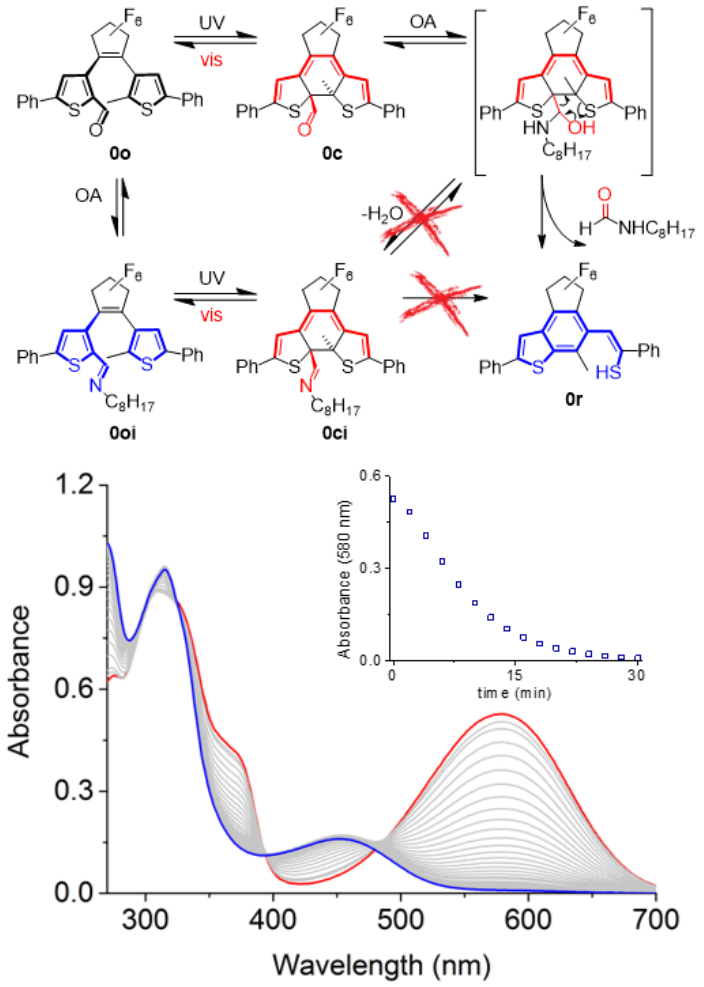


**Figure 2.** Proposed mechanism involving initial photoactivation of **Oo** and subsequent reaction of formed **Oc** with OA to yield rearrangement product **Or**. Bottom: Evolution of UV/vis absorption spectra after reaching the PSS at $\lambda_{irr}$ = 365 nm (red line, [**Oc**] = $3.6 \cdot 10^{-5}$ M in $CH_3CN$) upon addition of OA ($1.0 \cdot 10^{-2}$ M). The inset shows the decay of absorbance at $\lambda_{max}$ = 580 nm corresponding to the decreasing concentration of **Oc**.

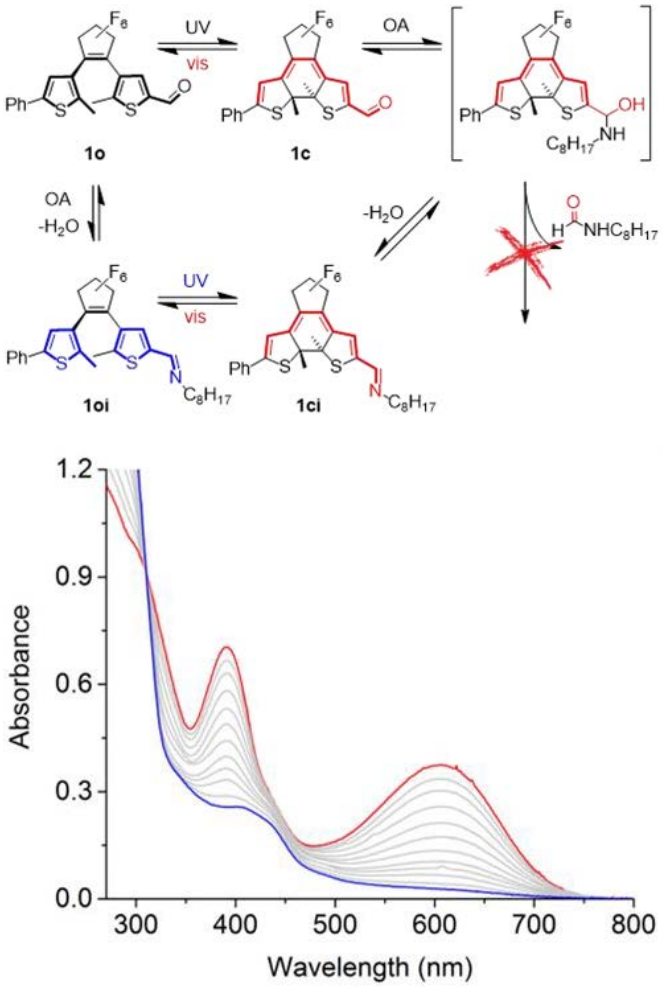


**Figure 3.** Proposed mechanism for reversible formation of imine-based DAEs **1ci** and **1oi**. Bottom: Evolution of UV/vis absorption spectra during reversible photoisomerization of **1ci** (red line, $5.5 \cdot 10^{-5}$ M in $CH_3CN$) to **1oi** (blue line) and *vice versa* upon irradiation ($\lambda_{irr}$ = 617 nm) and ($\lambda_{irr}$ = 302 nm), respectively

| analyte | rate constant ($min^{-1}$) with **probe**: | | | |
|---|---|---|---|---|
| | probe | | | |
| | **oc** | **4c** | **5c** | **6c** |
| 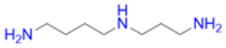 SPER | 0.98 | 1.78 | 1.55 | 2.64 |
|  CAD | 0.21 | 0.27 | 0.25 | 0.34 |
|  DAP | 0.79 | 1.52 | 1.20 | 3.41 |
| 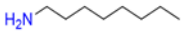 OA | 0.036 | 0.051 | 0.042 | 0.082 |
| 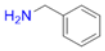 BA | 0.015 | 0.022 | 0.010 | 0.015 |

**Table 1**. Rate constants for the amine-induced rearrangement reaction representing the sensitivity of improved DAE-probes **4c-6c** in comparison to reference **Oc** [38] (all $2 \cdot 10^{-5}$ M) in presence of various amines ($5 \cdot 10^{-3}$ M).

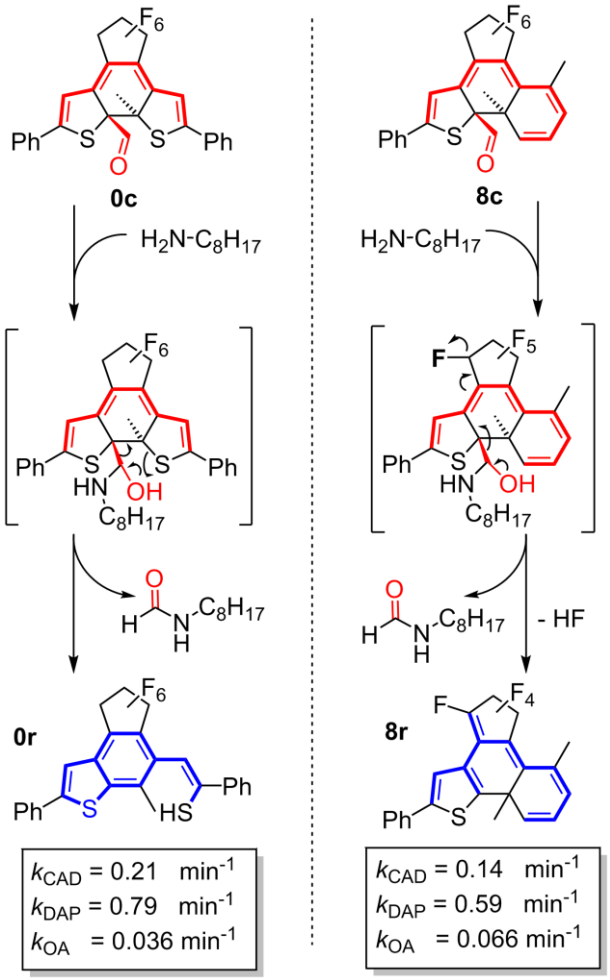


**Figure 4.** Comparison between the proposed mechanisms for the rearrangement of DAE-**Oc** and DAE-**8c** to **Or** and **8r**, respectively. Experimentally determined rate constants for **Oc** and **8c** in presence of different amines.

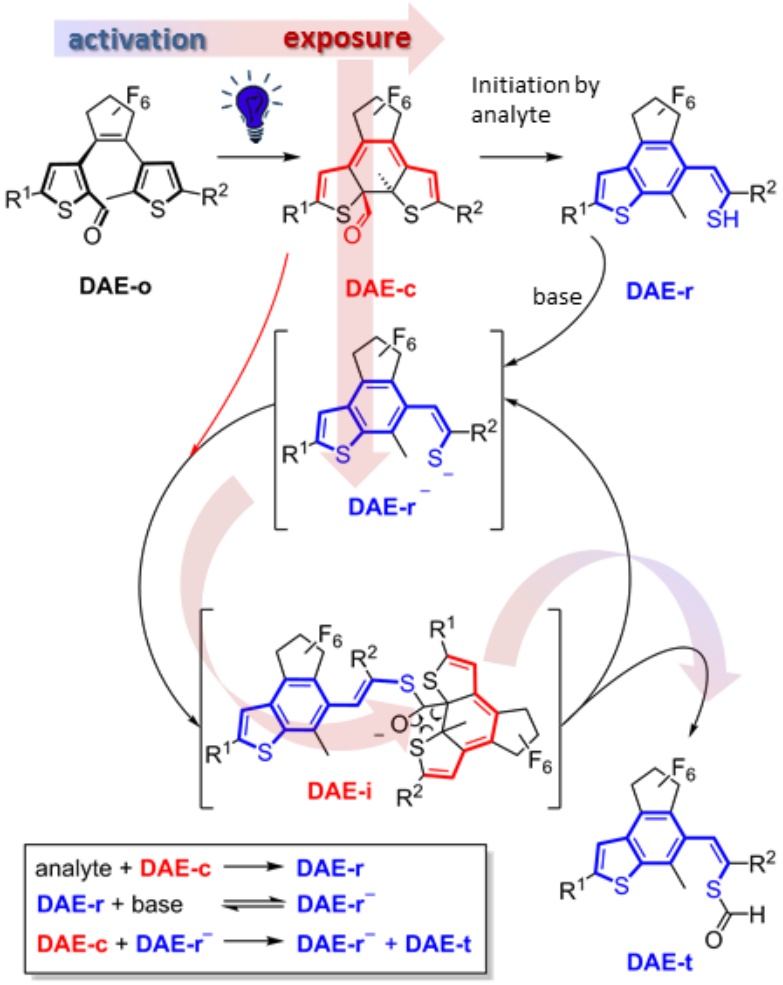


**Figure 5**. Proposed mechanism of the analyte-induced self-catalyzed rearrangement under basic conditions.

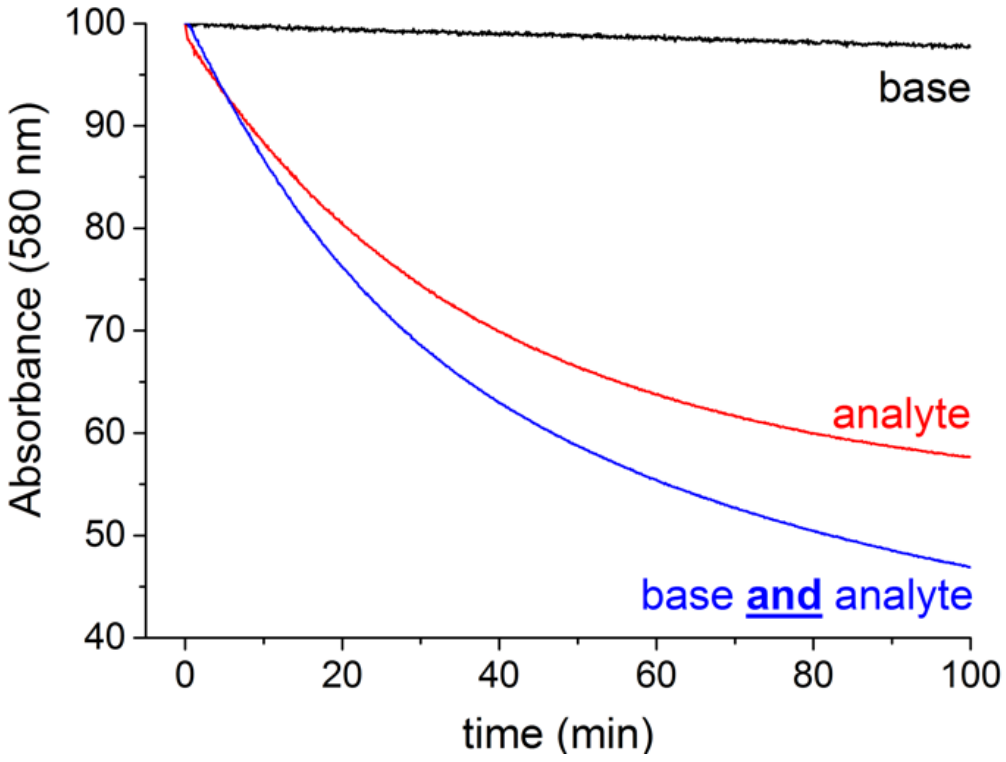


**Figure 6**. Decoloration rate of **Oc** ($6.5 \cdot 10^{-4}$ M in $CH_3CN$) with substoichiometric amounts of OA ($3.0 \cdot 10^{-4}$ M) in the absence (red) and presence (blue) of 1 vol% DMBA monitored by the absorbance decay at 580 nm. The control experiment contains a solution of **Oc** and DMBA only (black).

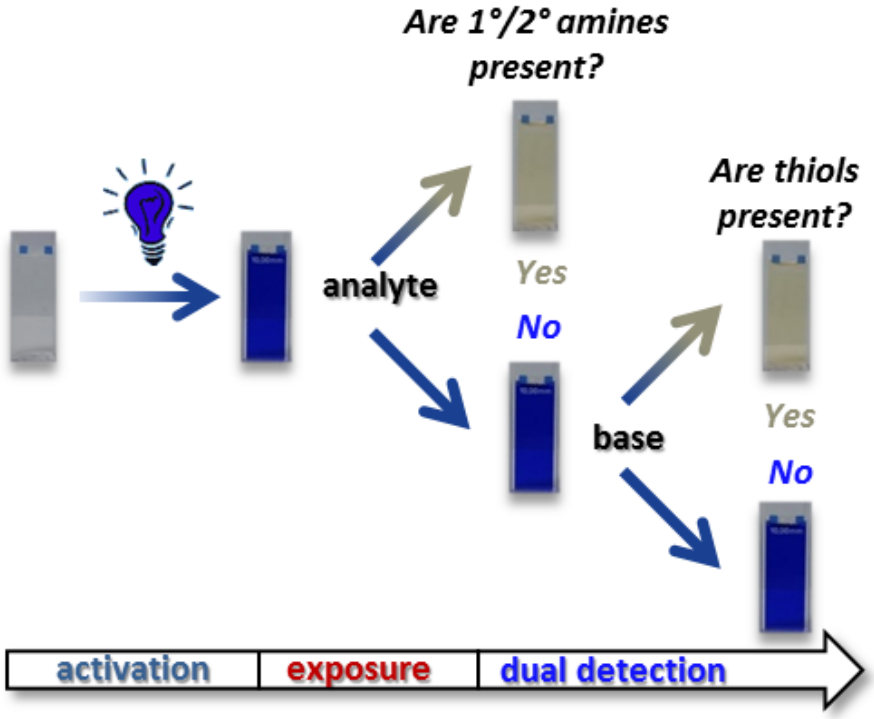


**Figure 7**. Sequential sensing scheme (flow chart) for the visual discrimination of primary/secondary amines and thiols employing the same DAE probe **6**.

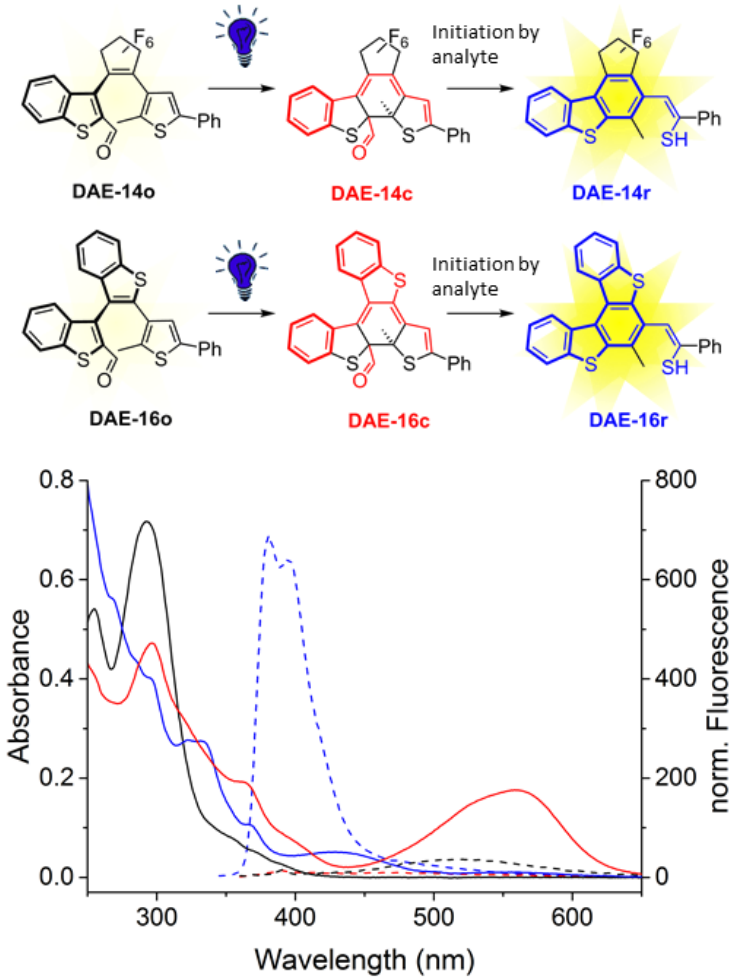


**Figure 8**. Top: Different forms of DAE probes **14** and **16**. Bottom: Absorption (solid lines) and emission spectra (dashed lines) of **16** ($4 \cdot 10^{-5}$ M in $CH_3CN$) in the open form (black), PSS mixture at 365 nm (red), and rearranged form originating from the PSS mixture (blue). Emission spectra were excited at 335 nm.

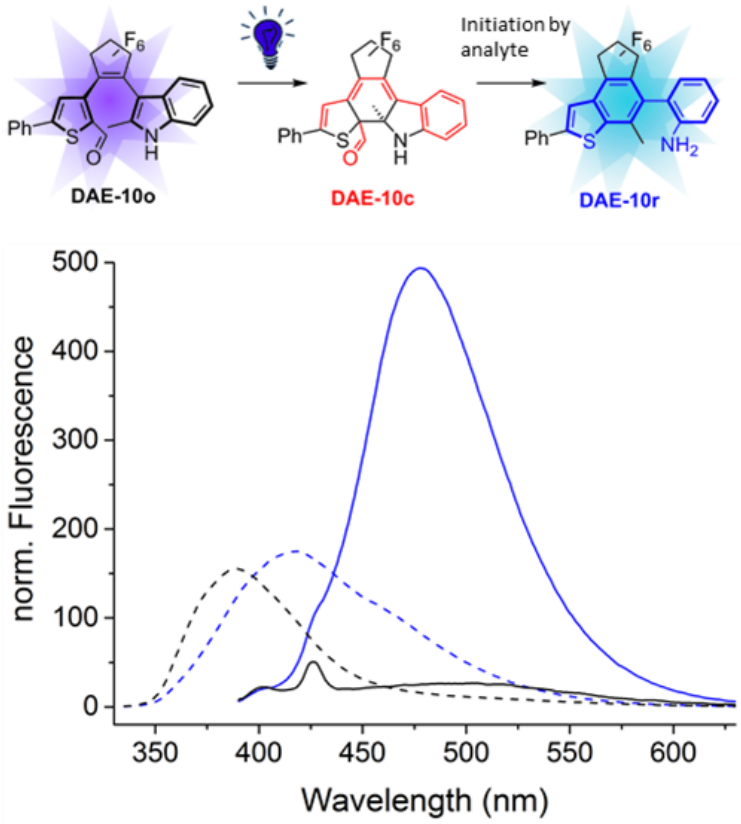


**Figure 9**. Top: Different forms of DAE probe **10**. Bottom: Emission spectra of **10** ($4 \cdot 10^{-5}$ M in *n*-hexane) in the open (black) and rearranged form (blue) upon excitation with 325 nm (dashed lines) and 380 nm (solid lines).